

## Article

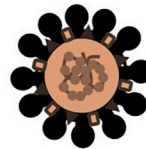
## Antiviral efficacy against and replicative fitness of an XBB.1.9.1 clinical isolate

**Comparison between XBB.1.5 and XBB.1.9.1****Antigenicity**

XBB.1.5



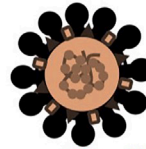
XBB.1.9.1

Both XBB.1.5 and XBB.1.9.1 **evade humoral immunity**.**Antiviral drug susceptibility**

XBB.1.5



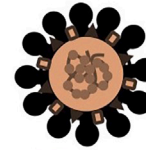
XBB.1.9.1

Remdesivir, molnupiravir, nirmatrelvir, and ensitrelvir are **effective**.**Growth capability in vivo**

XBB.1.5



XBB.1.9.1

XBB.1.5 and XBB.1.9.1 show **similar growth capability**.

Ryuta Uraki,  
Mutsumi Ito, Maki  
Kiso, ..., Hiroshi  
Yotsuyanagi, Ken  
Maeda, Yoshihiro  
Kawaoka

yoshihiro.kawaoka@wisc.edu

**Highlights**

The antigenicity of  
XBB.1.9.1 is similar to that  
of XBB.1.5

XBB.1.9.1 remains  
susceptible to antiviral  
drugs

The replicative ability of  
XBB.1.9.1 is comparable to  
that of XBB.1.5

Uraki et al., iScience 26, 108147  
November 17, 2023 © 2023 The  
Author(s).  
[https://doi.org/10.1016/  
j.isci.2023.108147](https://doi.org/10.1016/j.isci.2023.108147)

## Article

## Antiviral efficacy against and replicative fitness of an XBB.1.9.1 clinical isolate

Ryuta Uraki,<sup>1,2,9</sup> Mutsumi Ito,<sup>1,9</sup> Maki Kiso,<sup>1,9</sup> Seiya Yamayoshi,<sup>1,2,9</sup> Kiyoko Iwatsuki-Horimoto,<sup>1</sup> Yuko Sakai-Tagawa,<sup>1</sup> Masaki Imai,<sup>1,2</sup> Michiko Koga,<sup>3,4</sup> Shinya Yamamoto,<sup>1,4</sup> Eisuke Adachi,<sup>3</sup> Makoto Saito,<sup>3,4</sup> Takeya Tsutsumi,<sup>3,4</sup> Amato Otani,<sup>3</sup> Shuetsu Fukushi,<sup>5</sup> Shinji Watanabe,<sup>5</sup> Tadaki Suzuki,<sup>5</sup> Tetsuhiro Kikuchi,<sup>6</sup> Hiroshi Yotsuyanagi,<sup>3,4</sup> Ken Maeda,<sup>5</sup> and Yoshihiro Kawaoka<sup>1,2,7,8,10,\*</sup>

## SUMMARY

**The emergence and spread of new SARS-CoV-2 variants with mutations in the spike protein, such as the XBB.1.5 and XBB.1.9.1 sublineages, raise concerns about the efficacy of current COVID-19 vaccines and therapeutic monoclonal antibodies (mAbs). In this study, none of the mAbs we tested neutralized XBB.1.9.1 or XBB.1.5, even at the highest concentration used. We also found that the bivalent mRNA vaccine could enhance humoral immunity against XBB.1.9.1, but that XBB.1.9.1 and XBB.1.5 still evaded humoral immunity induced by vaccination or infection. Moreover, the susceptibility of XBB.1.9.1 to remdesivir, molnupiravir, nirmatrelvir, and ensitrelvir was similar to that of the ancestral strain and the XBB.1.5 isolate *in vitro*. Finally, we found the replicative fitness of XBB.1.9.1 to be similar to that of XBB.1.5 in hamsters. Our results suggest that XBB.1.9.1 and XBB.1.5 have similar antigenicity and replicative ability, and that the currently available COVID-19 antivirals remain effective against XBB.1.9.1.**

## INTRODUCTION

As of April 2023, XBB.1.5, a recombinant sublineage of the severe acute respiratory syndrome coronavirus 2 (SARS-CoV-2) B.1.1.529 (omicron) XBB subvariant, is currently dominant around the world. However, the prevalence of the XBB.1.9.1 sublineage is increasing in the United States (<https://covid.cdc.gov/covid-data-tracker/#variant-proportions>).

We and other groups have shown that XBB.1.5 is resistant to several therapeutic monoclonal antibodies and effectively evades humoral immunity elicited by natural infection or COVID-19 vaccinations.<sup>1–5</sup> In contrast, XBB.1.5 and the ancestral strain show similar susceptibility to drugs such as remdesivir (an RNA-dependent RNA polymerase (RdRp) inhibitor), molnupiravir (an RdRp inhibitor), and nirmatrelvir (a main protease inhibitor), which have all been authorized by the US Food and Drug Administration (FDA) for the treatment of COVID-19, and to ensitrelvir (a main protease inhibitor), which has been approved for emergency use in Japan for COVID-19 treatment.<sup>3</sup>

Although XBB.1.5 and XBB.1.9.1 possess the same amino acid substitutions in the spike protein, RdRp and main protease (Figure S1), there are additional amino acid substitutions in other virus proteins that may affect infectivity, viral replication, transmissibility and/or pathogenicity (Figure S1). Accordingly, we investigated vaccine efficacy against a clinical isolate of XBB.1.9.1, as well as the antiviral susceptibility and replicative fitness of the XBB.1.9.1 isolate *in vitro* or *in vivo*.

## RESULTS AND DISCUSSION

Efficacy of monoclonal antibodies against XBB.1.9.1 *in vitro* E6-TMPRSS2-T2A-ACE2 cells

As expected, due to the spike protein substitutions, we found that the reactivity of COVID-19 therapeutic monoclonal antibodies (mAbs) against XBB.1.9.1 (hCoV-19/Japan/TY41-951/2023) and XBB.1.5 (hCoV-19/USA/MD-HP40900-PIDYSWHNUB/2022) patient isolates was similar. None of the tested mAbs, including LYCoV1404 (marketed as bebtelovimab), REGN10987 (known as imdevimab), REGN10933 (known

<sup>1</sup>Division of Virology, Institute of Medical Science, University of Tokyo, Tokyo, Japan

<sup>2</sup>The Research Center for Global Viral Diseases, National Center for Global Health and Medicine Research Institute, Tokyo, Japan

<sup>3</sup>Department of Infectious Diseases and Applied Immunology, IMSUT Hospital of The Institute of Medical Science, University of Tokyo, Tokyo, Japan

<sup>4</sup>Division of Infectious Diseases, Advanced Clinical Research Center, Institute of Medical Science, University of Tokyo, Tokyo, Japan

<sup>5</sup>National Institute of Infectious Diseases, Tokyo, Japan

<sup>6</sup>Clinic of Nihon Sumo Kyokai, Tokyo, Japan

<sup>7</sup>Influenza Research Institute, Department of Pathobiological Sciences, School of Veterinary Medicine, University of Wisconsin-Madison, Madison, WI, USA

<sup>8</sup>The University of Tokyo, Pandemic Preparedness, Infection and Advanced Research Center (UTOPIA), Tokyo, Japan

<sup>9</sup>These authors contributed equally

<sup>10</sup>Lead contact

\*Correspondence: [yoshihiro.kawaoka@wisc.edu](mailto:yoshihiro.kawaoka@wisc.edu)

<https://doi.org/10.1016/j.isci.2023.108147>



as casirivimab), COV2-2196 (known as tixagevimab), COV2-2130 (known as cilgavimab), and S309 (known as the precursor of sotrovimab), neutralized the XBB.1.9.1 or XBB.1.5 isolate even at the highest concentration (>50,000 ng/mL) in Vero E6-TMPRSS2-T2A-ACE2 cells (Table 1).

### Neutralizing activity of plasma from vaccinees and patients against XBB.1.9.1

We also assessed neutralization of the XBB.1.9.1 isolate by using plasma obtained from three cohorts: (1) individuals who received a fourth dose of the monovalent mRNA vaccine, (2) individuals who received the bivalent mRNA vaccine as a fifth vaccine, and (3) vaccinees with BA.2 breakthrough infection after a third dose of the mRNA vaccine. The focus reduction neutralization test (FRNT<sub>50</sub>) geometric mean titers against XBB.1.9.1 were lower than those against the ancestral strain in plasma from all three cohorts (Figure 1A and Tables S1–S3). Consistent with our previous study, most samples of plasma from vaccinees with BA.2 breakthrough infection or from individuals who received the bivalent vaccine administered as a fifth dose had neutralizing activity and, samples from those who received a booster shot of the bivalent vaccine had increased neutralizing activity against XBB.1.9.1 (Figure 1B). This finding suggests that the bivalent vaccine can enhance humoral immunity, although XBB.1.9.1, as well as XBB.1.5, evades humoral immunity induced by mRNA vaccines or natural infection.

### Efficacy of antiviral drugs against XBB.1.9.1 in *vero* E6-TMPRSS2-T2A-ACE2 cells

Next, we examined the antiviral efficacy of four drugs, specifically, remdesivir, molnupiravir, nirmatrelvir, and ensitrelvir. We determined their *in vitro* 50% inhibitory concentration (IC<sub>50</sub>) values against the XBB.1.9.1 isolate. The susceptibilities of XBB.1.9.1 to these four antivirals were similar to those of the ancestral strain and those of the XBB.1.5 isolate (Figure 2). These results demonstrate that remdesivir, molnupiravir, nirmatrelvir, and ensitrelvir are effective against XBB.1.9.1 *in vitro*.

### Replicative fitness of XBB.1.9.1 compared with that of XBB.1.5 in hamsters

To further compare the replicative fitness of XBB.1.9.1 and XBB.1.5, we compared the growth of XBB.1.9.1 with that of XBB.1.5 in wild-type hamsters (Figure 3). Wild-type hamsters were intranasally inoculated with  $2 \times 10^5$  PFU of a mixture of XBB.1.9.1 and XBB.1.5 at ratios of 3:1 or 1:3. At 4 days post-infection, the proportion of each virus in the nasal turbinates and lungs of the infected hamsters was determined by using next-generation sequencing (NGS). NGS analysis revealed that the proportion of XBB.1.9.1 was similar in both the nasal turbinates and lungs of all infected animals to that in each inoculum for both ratios (Figure 3). Taken together, these results suggest that the antigenicity and replicative ability of XBB.1.9.1 are comparable to those of XBB.1.5.

Overall, our data suggest that bivalent mRNA vaccine boosters can enhance humoral immunity against the omicron sublineage XBB.1.9.1 and that remdesivir, molnupiravir, nirmatrelvir, and ensitrelvir remain effective *in vitro*. Considering the similar antigenicity and replicative ability of XBB.1.9.1 compared with XBB.1.5, it is likely that factors other than viral factors are responsible for the rising prevalence of XBB.1.9.1.

### Limitations of the study

We found that XBB.1.9.1 and XBB.1.5 have comparable replicative ability in naive wild-type hamsters. However, in the human population, many people possess SARS-CoV-2-specific adaptive immunity through natural infection and/or vaccination. Therefore, it remains uncertain whether the replicative ability of XBB.1.9.1 is comparable to that of XBB.1.5 in animals or humans with immunity to SARS-CoV-2. Given this uncertainty, it would be informative to compare the viral replicative ability of XBB.1.9.1 and XBB.1.5 in primary human airway/bronchial epithelial cells or airway organoids.<sup>1,6</sup>

## STAR★METHODS

Detailed methods are provided in the online version of this paper and include the following:

- KEY RESOURCES TABLE
- RESOURCE AVAILABILITY
  - Lead contact
  - Materials availability
  - Data and code availability
- EXPERIMENTAL MODEL AND STUDY PARTICIPANT DETAILS
- METHOD DETAILS
  - Cells
  - Viruses
  - Antibodies
  - Antiviral compounds
  - Focus reduction neutralization test (FRNT)
  - Inhibitory effect of compounds against SARS-CoV-2 *in vitro*
  - Experimental infection of Syrian hamsters
  - Whole genome sequencing
- QUANTIFICATION AND STATISTICAL ANALYSIS

**Table 1. Efficacy of monoclonal antibodies against omicron subvariants in vero E6-TMPRSS2-T2A-ACE2 cells<sup>a</sup>**

WHO label (Pango lineage)	Virus	Neutralization activity of monoclonal antibody — ng/ml <sup>b</sup>							
		REGN10987, imdevimab	REGN10933, casirivimab	COV2-2196, tixagevimab	COV2-2130, cilgavimab	S309, sotrovimab precursor	LYCoV1404, bebtelovimab	REGN10987 plus REGN10933	COV2-2196 plus COV2-2130
(A)	SARS-CoV-2/UT-NC002-1T/ Human/2020/Tokyo	89	64	64	152	5127	48	72	73
Omicron (XBB)	hCoV-19/Japan/TY41-795/2022	>50,000	>50,000	>50,000	>50,000	>50,000	>50,000	>50,000	>50,000
Omicron (XBB.1.5)	hCoV-19/USA/MD-HP40900- PIDYSWHNUB/2022	>50,000	>50,000	>50,000	>50,000	>50,000	>50,000	>50,000	>50,000
Omicron (XBB.1.9.1)	hCoV-19/Japan/TY41-951/2023	>50,000	>50,000	>50,000	>50,000	>50,000	>50,000	>50,000	>50,000

<sup>a</sup>The antibodies used in this analysis were produced in the authors' laboratories and are not identical to the commercially available products. Severe acute respiratory syndrome coronavirus 2 (SARS- CoV-2) variants are denoted according to the World Health Organization labels for the Pango lineage.

<sup>b</sup>The individual monoclonal antibodies were tested at a starting concentration of 50,000 ng/mL as a 50% focus reduction neutralization test (FRNT<sub>50</sub>) titer.

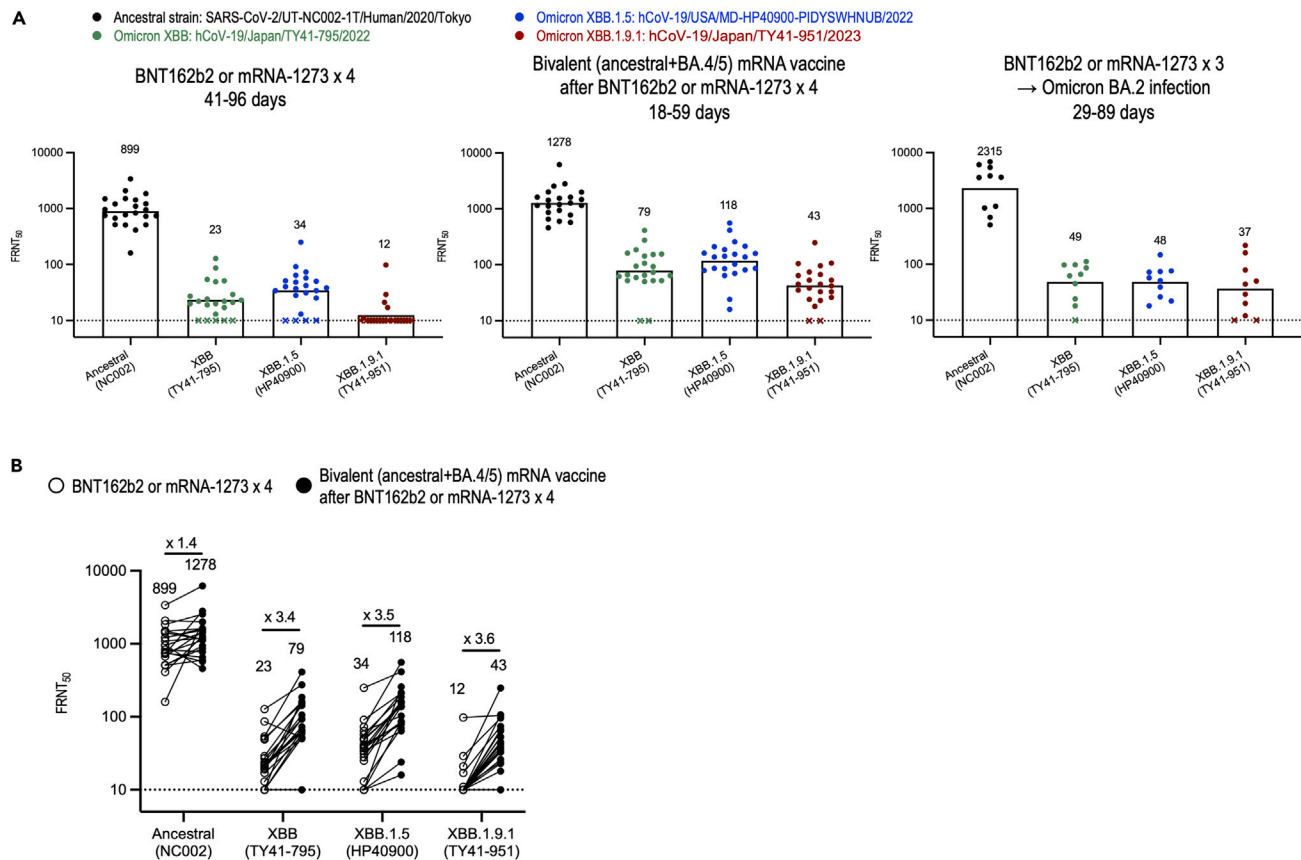


**Figure 1. In vitro neutralizing activity of plasma against SARS-CoV-2 omicron variants**

(A) Neutralizing titers of plasma samples obtained from individuals who had received four doses of BNT162b2 or mRNA-1273 vaccine ( $n = 22$ ), individuals immunized with the bivalent (ancestral and BA.4/5) vaccine as a fifth dose ( $n = 22$ ), and patients who were infected with the omicron BA.2 subvariant after receiving either the BNT162b2 or mRNA-1273 vaccine ( $n = 10$ ). Detailed information about the participants is provided in Tables S1–S3. FRNT50 values were determined in Vero E6-TMPRSS2-T2A-ACE2 cells. Each dot represents data from one individual. The lower limit of detection (value = 10) is indicated by the horizontal dashed line. Samples under the detection limit (<10-fold dilution) were assigned an FRNT50 of 10 and are represented by X. Geometric mean titers are shown.

(B) Neutralizing titers of plasma samples from the same individuals ( $n = 22$ ) after receiving four doses of BNT162b2 or mRNA-1273 vaccine compared with those after receiving the bivalent (ancestral and BA.4/5) vaccine as a fifth dose. Geometric mean titers are shown. Each line represents data from one individual.

## SUPPLEMENTAL INFORMATION

Supplemental information can be found online at <https://doi.org/10.1016/j.isci.2023.108147>.

## ACKNOWLEDGMENTS

We thank Susan Watson for scientific editing. We also thank Mashiho Yanagi, Kyoko Yokota, Kyoko Tada, Tomoka Nagashima, Naoko Mizutani, Rie Onoue, and Madoka Yoshikawa for technical assistance. Vero E6-TMPRSS2-T2A-ACE2 cells were provided by Dr. Barney Graham, NIAID Vaccine Research Center.

This study was supported by grants from the Center for Research on Influenza Pathogenesis and Transmission (75N93021C00014) by the National Institute of Allergy and Infectious Diseases, and a research program on emerging and re-emerging infectious diseases (JP21fk0108552), the Japan Program for Infectious Diseases Research and Infrastructure (JP23wm0125002), and the Japan Initiative for World-leading Vaccine Research and Development Centers (JP233fa627001) from the Japan Agency for Medical Research and Development. The funders had no role in the study design, data collection, data analysis, interpretation, or writing of the paper.

## AUTHOR CONTRIBUTIONS

R.U.: conceptualization, formal analysis, validation, visualization, and writing of the first draft. M. Ito, M. Kiso: data curation, formal analysis, and methodology. S. Yamayoshi: conceptualization, data curation, formal analysis, and methodology. K.I.H.: resources and validation. Y.S.-T., M.

## Vero E6-TMPRSS2-T2A-ACE2 cells

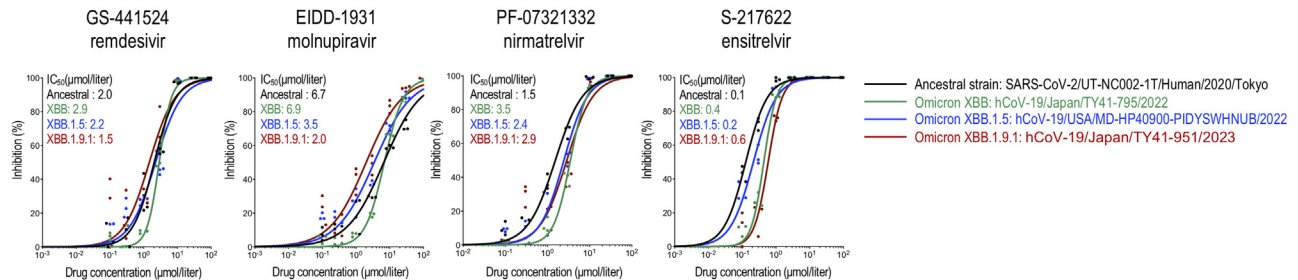


**Figure 2. *In vitro* inhibitory activity of antiviral drugs against Omicron subvariants**

The *in vitro* 50% inhibitory concentration ( $\text{IC}_{50}$ ) values were determined in Vero E6-TMPRSS2-T2A-ACE2 cells. GS-441524 (the main metabolite of remdesivir) and EIDD-1931 (the active form of molnupiravir) are RNA-dependent RNA polymerase inhibitors. PF-07321332 (nirmatrelvir) and S-217622 (ensitrelvir) are inhibitors of Mpro (also called 3CLpro). Data are the mean values for triplicate experiments. Statistical analysis of the data was not performed.

Imai, M. Koga, S. Yamamoto, E.A., M.S., T.T., A.O., T.K., H.Y.: resources. S.F., S.W., T.S., and K.M.: virus isolation and data curation. Y. Kawaoka: conceptualization, supervision, writing (review and editing), and funding acquisition. R.U., M. Ito, M. Kiso, and S. Yamayoshi contributed equally.

### DECLARATION OF INTERESTS

Y. Kawaoka has received unrelated funding support from Daiichi Sankyo Pharmaceutical, Toyama Chemical, Tauns Laboratories, Inc., Shionogi & Co. LTD, Otsuka Pharmaceutical, KM Biologics, Kyoritsu Seiyaku, Shinya Corporation, and Fuji Rebio. T.K. is employed by Nihon Sumo Kyokai.

Received: May 8, 2023

Revised: August 10, 2023

Accepted: October 2, 2023

Published: October 4, 2023

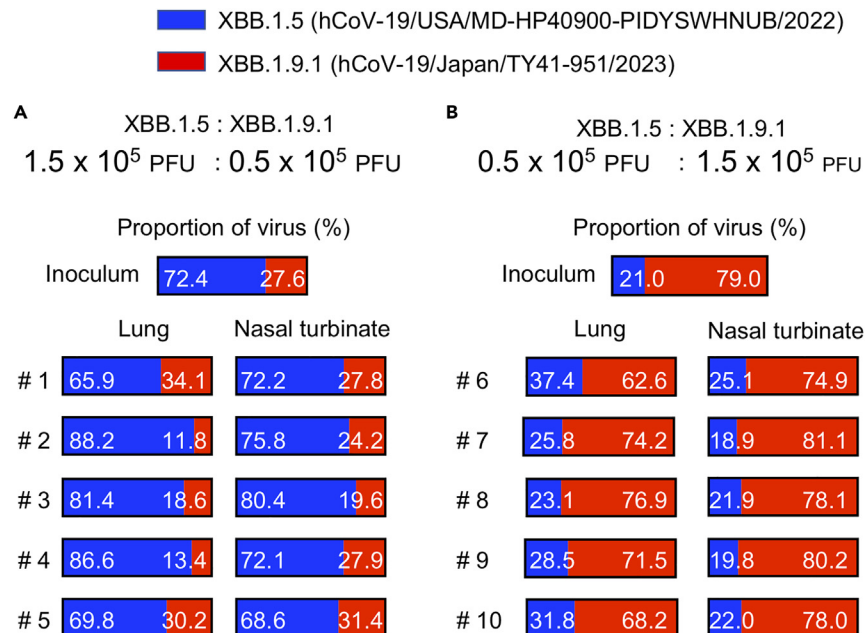


**Figure 3. Replicative fitness of XBB.1.9.1 compared with that of XBB.1.5 in hamsters**

XBB.1.5 and XBB.1.9.1 were mixed at 3:1 (A) or 1:3 (B) ratios on the basis of their infectious titer, and the virus mixture (total  $2 \times 10^5$  PFU in 60  $\mu\text{L}$ ) was intranasally inoculated into wild-type hamsters ( $n = 5$  per group). Nasal turbinates and lungs were collected from the infected animals at 4 dpi and analyzed by using NGS. The proportions of XBB.1.9.1 and XBB.1.5 were calculated from the four nucleotide differences in the ORF1a/b gene between the two viruses. Shown are the relative proportions of XBB.1.9.1 and XBB.1.5 in the infected animals.

**REFERENCES**

- Chen, J.J., Li, L.B., Peng, H.H., Tian, S., Ji, B., Shi, C., Qian, C., Jiang, W.G., Liu, M.C., Li, T.T., et al. (2023). Neutralization against XBB.1 and XBB.1.5 after omicron subvariants breakthrough infection or reinfection. *Lancet Reg. Health. West. Pac.* 33, 100759. <https://doi.org/10.1016/j.lanwpc.2023.100759>.
- Qu, P., Faraone, J.N., Evans, J.P., Zheng, Y.M., Carlin, C., Anghelina, M., Stevens, P., Fernandez, S., Jones, D., Panchal, A.R., et al. (2023). Enhanced evasion of neutralizing antibody response by Omicron XBB.1.5, CH.1.1, and CA.3.1 variants. *Cell Rep.* 42, 112443. <https://doi.org/10.1016/j.celrep.2023.112443>.
- Uraki, R., Ito, M., Kiso, M., Yamayoshi, S., Iwatsuki-Horimoto, K., Furusawa, Y., Sakai-Tagawa, Y., Imai, M., Koga, M., Yamamoto, S., et al. (2023). Antiviral and bivalent vaccine efficacy against an omicron XBB.1.5 isolate. *Lancet Infect. Dis.* 23, 402–403. [https://doi.org/10.1016/S1473-3099\(23\)00070-1](https://doi.org/10.1016/S1473-3099(23)00070-1).
- Uriu, K., Ito, J., Zahradnik, J., Fujita, S., Kosugi, Y., Schreiber, G., and Sato, K.; Genotype to Phenotype Japan G2P-Japan Consortium (2023). Enhanced transmissibility, infectivity, and immune resistance of the SARS-CoV-2 omicron XBB.1.5 variant. *Lancet Infect. Dis.* 23, 280–281. [https://doi.org/10.1016/S1473-3099\(23\)00051-8](https://doi.org/10.1016/S1473-3099(23)00051-8).
- Yue, C., Song, W., Wang, L., Jian, F., Chen, X., Gao, F., Shen, Z., Wang, Y., Wang, X., and Cao, Y. (2023). ACE2 binding and antibody evasion in enhanced transmissibility of XBB.1.5. *Lancet Infect. Dis.* 23, 278–280. [https://doi.org/10.1016/S1473-3099\(23\)00999\(23\)00010-5](https://doi.org/10.1016/S1473-3099(23)00999(23)00010-5).
- Muramoto, Y., Takahashi, S., Halfmann, P.J., Gotoh, S., Noda, T., and Kawaoka, Y. (2023). Replicative capacity of SARS-CoV-2 omicron variants BA.5 and BQ.1.1 at elevated temperatures. *Lancet. Microbe* 4, e486. [https://doi.org/10.1016/S2666-5247\(23\)00100-3](https://doi.org/10.1016/S2666-5247(23)00100-3).
- Takashita, E., Kinoshita, N., Yamayoshi, S., Sakai-Tagawa, Y., Fujisaki, S., Ito, M., Iwatsuki-Horimoto, K., Chiba, S., Halfmann, P., Nagai, H., et al. (2022). Efficacy of Antibodies and Antiviral Drugs against Covid-19 Omicron Variant. *N. Engl. J. Med.* 386, 995–998. <https://doi.org/10.1056/NEJMc2119407>.
- Takashita, E., Yamayoshi, S., Simon, V., van Bakel, H., Sordillo, E.M., Pekosz, A., Fukushi, S., Suzuki, T., Maeda, K., Halfmann, P., et al. (2022). Efficacy of Antibodies and Antiviral Drugs against Omicron BA.2.12.1, BA.4, and BA.5 Subvariants. *N. Engl. J. Med.* 387, 468–470. <https://doi.org/10.1056/NEJMc2207519>.
- Imai, M., Ito, M., Kiso, M., Yamayoshi, S., Uraki, R., Fukushi, S., Watanabe, S., Suzuki, T., Maeda, K., Sakai-Tagawa, Y., et al. (2023). Efficacy of Antiviral Agents against Omicron Subvariants BQ.1.1 and XBB. *N. Engl. J. Med.* 388, 89–91. <https://doi.org/10.1056/NEJMc2214302>.
- Uraki, R., Ito, M., Kiso, M., Yamayoshi, S., Iwatsuki-Horimoto, K., Sakai-Tagawa, Y., Imai, M., Koga, M., Yamamoto, S., Adachi, E., et al. (2023). Efficacy of antivirals and mRNA vaccination against an XBF clinical isolate. *Lancet Reg. Health. West. Pac.* 34, 100777. <https://doi.org/10.1016/j.lanwpc.2023.100777>.
- Matsuyama, S., Nao, N., Shirato, K., Kawase, M., Saito, S., Takayama, I., Nagata, N., Sekizuka, T., Katoh, H., Kato, F., et al. (2020). Enhanced isolation of SARS-CoV-2 by TMPRSS2-expressing cells. *Proc. Natl. Acad. Sci. USA* 117, 7001–7003. <https://doi.org/10.1073/pnas.2002589117>.
- Imai, M., Halfmann, P.J., Yamayoshi, S., Iwatsuki-Horimoto, K., Chiba, S., Watanabe, T., Nakajima, N., Ito, M., Kuroda, M., Kiso, M., et al. (2021). Characterization of a new SARS-CoV-2 variant that emerged in Brazil. *Proc. Natl. Acad. Sci. USA* 118, e2106535118. <https://doi.org/10.1073/pnas.2106535118>.
- Vanderheiden, A., Edara, V.V., Floyd, K., Kauffman, R.C., Mantus, G., Anderson, E., Roupael, N., Edupuganti, S., Shi, P.Y., Menachery, V.D., et al. (2020). Development of a Rapid Focus Reduction Neutralization Test Assay for Measuring SARS-CoV-2 Neutralizing Antibodies. *Curr. Protoc. Immunol.* 131, e116. <https://doi.org/10.1002/cpim.116>.
- Takashita, E., Morita, H., Ogawa, R., Nakamura, K., Fujisaki, S., Shirakura, M., Kuwahara, T., Kishida, N., Watanabe, S., and Odagiri, T. (2018). Susceptibility of Influenza Viruses to the Novel Cap-Dependent Endonuclease Inhibitor Baloxavir Marboxil. *Front. Microbiol.* 9, 3026. <https://doi.org/10.3389/fmicb.2018.03026>.



STAR★METHODS

KEY RESOURCES TABLE

REAGENT or RESOURCE	SOURCE	IDENTIFIER
<b>Antibodies</b>		
Tixagevimab	Takashita et al. <sup>7</sup>	NA
Casirivimab	Takashita et al. <sup>7</sup>	NA
Cilgavimab	Takashita et al. <sup>7</sup>	NA
Imdevimab	Takashita et al. <sup>7</sup>	NA
S309	Takashita et al. <sup>7</sup>	NA
bebtelovimab	Takashita et al. <sup>8</sup>	NA
SARS-CoV-2 nucleoprotein (clone N45)	TAUNS Laboratories, Inc.	NA
Peroxidase AffiniPure Goat Anti-Mouse IgG (H+L)	Jackson ImmunoResearch Laboratories Inc.	Cat#115-035-003; RRID:AB_10015289
<b>Bacterial and virus strains</b>		
hCoV-19/Japan/TY41-951/2023	This study	N/A
hCoV-19/USA/MD-HP40900-PIDYSWHNUB/2022	Uraki et al. <sup>3</sup>	N/A
hCoV-19/Japan/TY41-795/2022	Imai et al. <sup>9</sup>	N/A
SARS-CoV-2/UT-NC002-1T/Human/2020/Tokyo	Takashita et al. <sup>7</sup>	N/A
<b>Biological samples</b>		
Human sera	Uraki et al. <sup>10</sup>	N/A
<b>Chemicals, peptides, and recombinant proteins</b>		
Dulbecco's modified Eagle's medium (DMEM)	SIGMA	Cat #D5796
Fetal Calf Serum (FCS)	gibco	Cat #10437-028
penicillin–streptomycin	FUJIFILM Wako Pure Chemical Corporation	Cat #168-23191
Puromycin	InvivoGen	Cat # ant-pr-1
Geneticin	InvivoGen	Cat # ant-gn-5
plasmocin prophylactic	InvivoGen	Cat #ant-mpp
Expi293 expression medium	Thermo Fisher Scientific	Cat # A1435101
GS-441524	MedChemExpress	Cat # HY-103586
EIDD-1931	MedChemExpress	Cat # HY-125033
PF-07321332	MedChemExpress	Cat # HY-138687
S-217622	Shionogi & Co., Ltd.	N/A
Methyl Cellulose 400	FUJIFILM Wako Pure Chemical Corporation	Cat # 132-05055
<b>Deposited data</b>		
the variable region of the heavy and light chains of tixagevimab	PDB	QLI33947 and QLI33948
the variable region of the heavy and light chains of casirivimab	PDB	6XDG_B and 6XDG_D
the variable region of the heavy and light chains of cilgavimab	PDB	QKY76296 and QKY75909
the variable region of the heavy and light chains of imdevimab	PDB	6XDG_A and 6XDG_A
the variable region of the heavy and light chains of S309	PDB	6WS6_A and 6WS6_F
the variable region of the heavy and light chains of bebtelovimab	PDB	7MMO_D and 7MMO_E
the constant gamma heavy chain coding sequences	UniProtKB/Swiss-Prot	P01857
the constant kappa light chain coding sequences	UniProtKB/Swiss-Prot	P01834

(Continued on next page)



**Continued**

REAGENT or RESOURCE	SOURCE	IDENTIFIER
the constant lambda light chain coding sequences	UniProtKB/Swiss-Prot	P0DOY2
hCoV-19/Japan/TY41-951/2023 (XBB.1.9.1) sequence	the Global Initiative on Sharing All Influenza Data (GISAI) database	EPI_ISL_17482300
Wuhan/Hu-1/2019 sequence	GenBank	MN908947
<b>Experimental models: Cell lines</b>		
VeroE6/TMPRSS2 cells	JCRB Cell Bank	JCRB1819
Vero E6-TMPRSS2-T2A-ACE2 cells	Graham laboratory	NA
Chinese hamster ovary (CHO) cells	GenScript	NA
Expi293F cells	Thermo Fisher Scientific	Cat# A14527
<b>Experimental models: Organisms/strains</b>		
Slc:Syrian hamsters (male, 6 weeks old)	Japan SLC Inc.	<a href="http://www.jslc.co.jp/pdf/data/2013/syrian2013.pdf">http://www.jslc.co.jp/pdf/data/2013/syrian2013.pdf</a>
<b>Software and algorithms</b>		
GraphPad Prism 9.3.0	GraphPad Software, Inc.	<a href="https://www.graphpad.com/scientific-software/prism/">https://www.graphpad.com/scientific-software/prism/</a>
BioSpot software	Cellular Technology	<a href="https://immunospot.com/plaque-colony-counting">https://immunospot.com/plaque-colony-counting</a>
<b>Other</b>		
QIAamp Viral RNA Mini Kit	QIAGEN	Cat# 52926
LunarScript RT SuperMix Kit	New England BioLabs	Cat# E3010
Q5 High-Fidelity DNA polymerase	New England BioLabs	Cat# M0491
Q5 Hot Start DNA polymerase	New England BioLabs	Cat# M0493
QIAseq FX DNA Library Kit	QIAGEN	Cat# 180477

**RESOURCE AVAILABILITY**

**Lead contact**

Further information or requests should be directed to and will be fulfilled by the Lead Contact, Yoshihiro Kawaoka ([yoshihiro.kawaoka@wisc.edu](mailto:yoshihiro.kawaoka@wisc.edu)).

**Materials availability**

All materials can be obtained directly from the authors or through commercially available sources, with the exception of clinical specimens. Due to the extremely limited availability of these clinical specimens, we are unable to provide them.

**Data and code availability**

- All data used in this paper are available in the main text, in the [supplemental information](#), or the sources have been clearly stated.
- This paper does not report original code.
- Any additional information required to reanalyze the data reported in this paper is available from the [lead contact](#) upon request.

**EXPERIMENTAL MODEL AND STUDY PARTICIPANT DETAILS**

Animal studies were carried out in accordance with the recommendations in the Guide for the Care and Use of Laboratory Animals of the National Institutes of Health. The protocols were approved by the Animal Experiment Committee of the Institute of Medical Science, the University of Tokyo (approval number PA19-75). Virus inoculations were performed under isoflurane, and all efforts were made to minimize animal suffering.

To collect and use clinical specimens, the research protocol was approved by the Research Ethics Review Committee of the Institute of Medical Science of the University of Tokyo (approval numbers: 2019-71-0201 and 2020-740226). After informed consent was obtained, plasma specimens were collected from COVID-19 convalescent individuals and vaccinees.

## METHOD DETAILS

### Cells

Vero E6-TMPRSS2-T2A-ACE2 cells were cultured in Dulbecco's modified Eagle's medium (DMEM) containing 10% Fetal Calf Serum (FCS), 100 U/mL penicillin–streptomycin, and 10 µg/mL puromycin. VeroE6/TMPRSS2 (JCRB 1819) cells<sup>11,12</sup>(Imai et al., 2021; Matsuyama et al., 2020)(Matsuyama, Nao et al. 2020, Imai, Halfmann et al. 2021)(Imai et al., 2021; Matsuyama et al., 2020)(Imai et al., 2021; Matsuyama et al., 2020)(Imai et al., 2021; Matsuyama et al., 2020) were propagated in the presence of 1 mg/ml geneticin (G418; Invivogen) and 5 µg/ml plasmodin prophylactic (Invivogen) in DMEM containing 10% FCS. Vero E6-TMPRSS2-T2A-ACE2 and VeroE6/TMPRSS2 cells were maintained at 37°C with 5% CO<sub>2</sub>. Chinese hamster ovary (CHO) cells were maintained in DMEM containing 10% FCS and antibiotics at 37°C with 5% CO<sub>2</sub>. Expi293F cells (Thermo Fisher Scientific) were maintained in Expi293 expression medium (Thermo Fisher Scientific) at 37°C under 8% CO<sub>2</sub>. The cells were regularly tested for mycoplasma contamination by using PCR, and confirmed to be mycoplasma-free.

### Viruses

The SARS-CoV-2 viruses hCoV-19/Japan/TY41-951/2023 (Omicron XBB.1.9.1; isolated using Vero E6-TMPRSS2-T2A-ACE2 cells), hCoV-19/USA/MD-HP40900-PIDYSWHNUB/2022 (Omicron XBB.1.5)<sup>3</sup>, hCoV-19/Japan/TY41-795/2022 (Omicron XBB)<sup>9</sup> and SARS-CoV-2/UT-NC002-1T/Human/2020/Tokyo<sup>7</sup> (ancestral strain) were propagated in VeroE6/TMPRSS2 cells.

All experiments with SARS-CoV-2 were performed in enhanced biosafety level 3 containment laboratories at the University of Tokyo and the National Institute of Infectious Diseases, Japan, which are approved for such use by the Ministry of Agriculture, Forestry, and Fisheries, Japan.

### Antibodies

Amino acid sequences for the variable region of the heavy and light chains of the following human monoclonal antibodies against the S protein were used for gene synthesis: clones tixagevimab (COV2-2196/AZD8895; GenBank accession numbers QLI33947 and QLI33948), casirivimab (REGN10933; PDB accession numbers 6XDG\_B and 6XDG\_D), cilgavimab (COV2-2130/AZD1061; GenBank accession numbers QKY76296 and QKY75909), imdevimab (REGN10987; PDB accession numbers 6XDG\_A and 6XDG\_A), S309 (PDB accession numbers 6WS6\_A and 6WS6\_F), and bebtelovimab (LYCoV1404; PDB accession numbers 7MMO\_D and 7MMO\_E). An artificial signal sequence and the constant gamma heavy (IgG1, UniProtKB/Swiss-Prot accession number P01857) and kappa (UniProtKB/Swiss-Prot accession number P01834) or lambda (UniProtKB/Swiss-Prot accession number P0DOY2) light chain coding sequences were added before and after each variable region. Codon usage was optimized for expression in CHO cells. The synthesized genes were cloned into a plasmid for protein expression and transfected into CHO cells. Cell culture media were harvested after incubation for 10–14 days at 37°C. Monoclonal antibodies were purified by using MabSelect SuRe LX (Cytiva) or a protein A column. Purity was confirmed by SDS-PAGE and/or HPLC before use. The reactivities of these antibodies against SARS-CoV-2, including the Alpha, Beta, Delta, Gamma, and Omicron variants, have been tested previously.<sup>7</sup>

### Antiviral compounds

Active components of remdesivir and molnupiravir (i.e., GS-441524 and EIDD-1931), and nirmatrelvir (PF-07321332) were purchased from MedChemExpress. Ensitrelvir (S-217622) was kindly provided by Shionogi & Co., Ltd. All compounds were dissolved in dimethyl sulfoxide.

### Focus reduction neutralization test (FRNT)

Neutralization activities of monoclonal antibodies and human plasma were determined by using a focus reduction neutralization test as previously described.<sup>13</sup> Serially diluted antibodies (starting concentration, 50,000 ng/ml) were mixed with 100–400 focus-forming units (FFU) of virus/well and incubated for 1 h at 37°C. The antibody-virus mixture (50µl) was then inoculated onto Vero E6-TMPRSS2-T2A-ACE2 cells in 96-well plates in triplicate. After a 1-h incubation at 37°C, 100µl of 1.5% Methyl Cellulose 400 (FUJIFILM Wako Pure Chemical Corporation, Japan) in culture medium was added to each well. The cells were incubated for 14–18 h at 37°C and then fixed with formalin. For human plasma, the samples were first incubated at 56°C for 1 h. Then, the treated plasma samples were serially diluted five-fold with DMEM containing 2% FCS in 96-well plates and mixed with 100–400 FFU of virus/well, followed by incubation at 37°C for 1 h. The plasma-virus mixture was inoculated onto Vero E6-TMPRSS2-T2A-ACE2 cells in 96-well plates in duplicate. After a 1-h incubation at 37°C, 100µl of 1.5% Methyl Cellulose 400 (FUJIFILM Wako Pure Chemical Corporation) in culture medium was then added to each well. The cells were incubated for 14–18 h at 37°C and then fixed with formalin.

After the formalin was removed, the cells were immunostained with a mouse monoclonal antibody against SARS-CoV-2 nucleoprotein [N45 (TAUNS Laboratories, Inc., Japan)], followed by a horseradish peroxidase-labeled goat anti-mouse immunoglobulin (Jackson ImmunoResearch Laboratories Inc.). The infected cells were stained with TrueBlue Substrate (SeraCare Life Sciences) and then washed with distilled water. After cell drying, the focus numbers were quantified by using an ImmunoSpot S6 Analyzer, ImmunoCapture software, and BioSpot software (Cellular Technology). The results are expressed as the 50% focus reduction neutralization titer (FRNT<sub>50</sub>). The FRNT<sub>50</sub> values were calculated by using GraphPad Prism (GraphPad Software). Samples under the detection limit (<10-fold dilution) were assigned an FRNT<sub>50</sub> value of 10.

### **Inhibitory effect of compounds against SARS-CoV-2 *in vitro***

Antiviral susceptibilities of SARS-CoV-2 were determined by applying a focus reduction assay as previously described.<sup>9,14</sup> Vero E6-TMPRSS2-T2A-ACE2 cells in 96-well plates were infected with 100–400 FFU of virus/well. Virus adsorption was carried out for 1 h at 37°C and then the inoculum was removed and 1% Methyl Cellulose 400 (FUJIFILM Wako Pure Chemical Corporation) in culture medium containing serial dilutions of antiviral compounds was added to each well in triplicate. The cells were incubated for 18 h at 37°C and then fixed with formalin. After the formalin was removed, immunostaining was performed as described for the FRNT. The results are expressed as the 50% inhibitory concentration (IC<sub>50</sub>). The IC<sub>50</sub> values were calculated by using GraphPad Prism (GraphPad Software).

### **Experimental infection of Syrian hamsters**

XBB.1.9.1 was mixed with XBB.1.5 at a 1:3 or 3:1 ratio on the basis of their titers, and each virus mixture (total  $2 \times 10^5$  PFU in 60  $\mu$ L) was inoculated into five six-week-old male wild-type hamsters. At 4 days post-infection, five animals were euthanized and nasal turbinates and lungs were collected.

### **Whole genome sequencing**

Viral RNA was extracted by using a QIAamp Viral RNA Mini Kit (QIAGEN). The whole genome of SARS-CoV-2 was amplified by using a modified ARTIC network protocol in which some primers were replaced or added. Briefly, viral cDNA was synthesized from the extracted RNA by using a LunaScript RT SuperMix Kit (New England BioLabs). The DNA was amplified by performing a multiplexed PCR in two pools using the ARTIC-N5 primers and the Q5 High-Fidelity DNA polymerase or Q5 Hot Start DNA polymerase (New England BioLabs). The DNA libraries for Illumina NGS were prepared from pooled amplicons by using a QIAseq FX DNA Library Kit (QIAGEN) and were then analyzed by using the MiSeq (Illumina) or iSeq 100 System (Illumina). To determine the virus sequences, the reads were assembled by CLC Genomics Workbench (version 22, Qiagen) with the Wuhan/Hu-1/2019 sequence (GenBank accession no. MN908947) as a reference. The sequences of XBB.1.9.1 (hCoV-19/Japan/TY41-951/2023) was deposited in the Global Initiative on Sharing All Influenza Data (GISAID) database with accession ID: EPI\_ISL\_17482300.

For the analysis of the XBB.1.9.1:XBB.1.5 ratio after co-infection, the ratio of XBB.1.9.1 to XBB.1.5 was calculated from the four nucleotide differences in the ORF1a/b gene between the two viruses. Samples with more than 1000 read-depths were analyzed.

### **QUANTIFICATION AND STATISTICAL ANALYSIS**

We used GraphPad Prism 9.3.0 for data visualization to determine the FRNT<sub>50</sub> and IC<sub>50</sub> values.